JOC The Journal of Organic Chemistry

pubs.acs.org/joc Article

Nucleophilicity and Electrophilicity in the Gas Phase: Silane Hydricity

Allison E. Krajewski and Jeehiun K. Lee*

Cite This: J. Org. Chem. 2022, 87, 1840−1849 Read Online

ACCESS | Metrics & More | Article Recommendations | Supporting Information

ABSTRACT: Hydricity is of great import as hydride transfer reactions are prominent in many processes, including organic synthesis, photoelectrocatalysis, and hydrogen activation. Herein, the kinetic hydricity of a series of silanes is examined in the gas phase. Most of these reactions have not heretofore been studied *in vacuo* and provide valuable data that can be compared to condensed-phase hydricity, to reveal the effects of solvent. Both experiments and computations are used to gain insight into mechanism and reactivity. In a broader sense, these studies also represent a first step toward systematically understanding nucleophilicity and electrophilicity in the absence of a solvent.

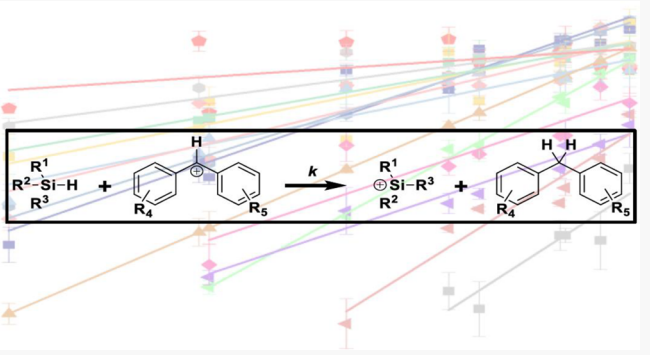

INTRODUCTION

The hydride ion (H^-) is the simplest Lewis base and plays important roles in both biological and organic processes. Biologically, for example, nicotinamide adenine dinucleotide phosphate (NADH) and flavin adenine dinucleotide ($FADH_2$) are important enzymatic cofactors that donate hydride.[1,2] In organic chemistry, hydride transfer is a key step in many synthetic reactions, and metal hydrides are widely used as reducing agents.[3] More recently, metal-free hydride donors have come to the forefront of the field; one class of metal-free hydrides consists of silanes, which are useful in a myriad of reactions, including in the reduction of aldehydes and ketones,[4,5] as frustrated Lewis pairs in hydrogen activation,[6,7] and as catalysts in the reduction of carbon dioxide.[8−15]

Quantifying hydricity is important for experimental design. Thermodynamic hydricity is an absolute scale that measures the Gibbs free energy change (ΔG_{H^-}) for the dissociation of a hydride donor (RH) into a hydride ion (H^-) and a hydride acceptor (R^+) (eq 1).

$$RH \rightarrow H^- + R^+ \quad (\Delta G_{H^-}) \tag{1}$$

There are several ways to measure thermodynamic hydricity, some of which can be experimentally challenging; they have been reviewed previously.[14−16]

Kinetic hydricity can be ascertained from the rate constants of various reactions involving hydride abstraction. The broadest study of kinetic hydricity has been undertaken by Mayr and co-workers over more than 30 years.[17−25] In the Mayr work, hydricity is assessed as nucleophilicity; Mayr has examined nucleophilicity and electrophilicity extensively, where reactivity follows a linear free energy relationship (eq 2).[18,23,26]

$$\log(k) = s_N(N + E) \tag{2}$$

where k is the rate of the reaction, s_N is a nucleophilic slope/sensitivity parameter, N is a nucleophilicity parameter, and E is an electrophilicity parameter. The nucleophilicity/electrophilicity scales describing hydricity were developed for reactions conducted in the condensed phase, using substituted benzhydryl cations as the original series of reference acceptors (electrophiles).[18−20] These benzhydryl cations can be "tuned" by modifying substituents on the aryl rings in different positions, allowing for study over a wide reactivity range.

Herein, building on prior preliminary work, we examine a large set of silanes and their reactivity toward a series of benzhydryl cations.[27] By studying these reactions in the gas phase, we can eliminate the influence of underlying solvent effects and evaluate the intrinsic properties of these species and attendant reactions. Comparison to condensed-phase data can then reveal effects of media. This study is important for improving our understanding of not only hydricity but also, in a broader sense, nucleophilicity and electrophilicity and the influence of a solvent on these fundamental properties.

Special Issue: Solvation Effects in Organic Chemistry

Received: November 11, 2021
Published: January 19, 2022

https://doi.org/10.1021/acs.joc.1c02763
J. Org. Chem. 2022, 87, 1840−1849

RESULTS

Experimental Results: Abstraction of Hydride from Silanes. To ascertain hydricity, we studied the reactions between a series of silanes and benzhydryl cations (Figure 1). We track, via mass spectrometry, the disappearance of electrophilic benzhydryl cation **1** and the appearance of the silyl cation product shown in Figure 1.

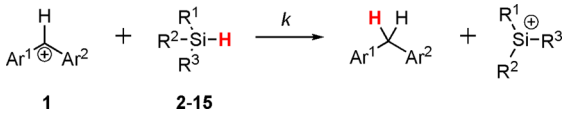

1 2-15

Figure 1. Reactions studied herein.

The electrophiles (Figure 2) were chosen to allow for variation in fluorine substitution and to include electrophiles that have also been studied in solution by the Mayr group.[18−20,24,25]

The silane nucleophiles (hydride donors) are a mix of straight chain versus branched alkyl substitution, phenyl substitution, and oxygen substitution (Figure 3).

The rate constants for the reactions of benzhydryl cations **1** with silanes **2**−**15** are compiled in Table 1. A few of these reactions were studied in our prior work, as indicated in Table 1.[27]

With rate constants (Table 1) in hand, we compile a "Mayr-type" plot, graphing the log of the rate constants for the reaction between the series of nucleophiles and electrophiles (y-axis) versus the log of the rate constants of the electrophiles with triisopropylsilane (iPr$_3$SiH, **12**) as our reference nucleophile (x-axis) (Figure 4; linear regression and correlation coefficients for all figures are available in the Supporting Information). Because we are still in the early stages of this research, we are not yet deriving specific parameters, but we are interpreting the data in a correlative fashion with respect to Mayr.

Further interpretation of these data will follow; we will next describe additional studies of the reaction mechanism.

Reaction Details: Mechanistic Studies. *Reaction Paths.* We are always concerned with this type of reaction, that hydride transfer (path A, Figure 5) is taking place, not a proton transfer to yield a carbene (path B, Figure 5).

To ascertain the probability of one path over the other, we conducted calculations for both paths, for the reaction of benzhydryl cation **1** with reference silane **12**.[28] As a first pass, we calculated the ΔG, just to ascertain the thermochemistry of the reaction (Table 2). Of course, the rates of the experimental reactions are dependent on kinetics, but we first calculated the exergonicity and/or endergonicity. We have long found that B3LYP/6-31+G(d) can be quite accurate for our organic systems, based on benchmarking with experimental values.[29−35] We calculated ΔG using both B3LYP/6-31+G(d) and B3LYP-D3(BJ)/6-311++G(2d,p), to account for dispersion and to utilize a larger basis set for the silicon. From Table 2, one can see that the two methods yield quite comparable values. For path A, ΔG is always negative [ranging from −1.9 to −32.0 kcal mol^{-1} at B3LYP-D3(BJ)/6-311++G(2d,p)], whereas for path B, whether the singlet or triplet carbene is formed, the reactions are very endergonic (ΔG ranges from 39.3 to 74.0 kcal mol^{-1} for these reactions). ΔG is so vastly different for paths A and B that by the Hammond postulate one would hypothesize that the barrier for path A would also be significantly lower than that for path B. To support this hypothesis, we also calculated the barriers for the reaction of the parent benzhydryl cation **1h** with silanes **3** and **12**. In both cases, we find that the barrier for path A is 70 kcal mol^{-1} more favorable than that for path B, comparable to the differences in ΔG.[36]

Hammett Studies. We also conducted a Hammett analysis, to ensure that we were not seeing any unexpected changes in the mechanism or rate-determining step in the course of our studies.[37,38] We selected two well-behaved silanes, which have "middle-of-the-road" rate constants: **4** (nPr$_3$SiH) and **8** (iBu$_3$SiH). Also, one has straight, while the other has branched, alkyl chain substitution. We allowed these silanes to react with a series of substituted benzhydryl cations (Figure 6), which have both classic electron-withdrawing and electron-donating groups.

The resultant Hammett plots are linear, with positive slopes (Figure 7; linear regression and correlation coefficients for all figures are available in the Supporting Information). The linearity of the plots indicates no change in the rate-determining step or mechanism for these reactions. The upward slope is consistent with the decrease in positive charge at the benzhydryl cation center. The slope is roughly 1, indicating that the reaction is reasonably sensitive to the aryl substitution. All of this is consistent with the hydride transfer reaction depicted in Figure 1.[39]

DISCUSSION

Gas-Phase Hydricity Trends. Figure 4 shows all of the data collected for the reactions between the silanes and benzhydryl cations. In this Mayr-type plot, the x-axis represents the log of the rate constant of the reaction of each benzhydryl cation electrophile with the reference silane nucleophile, **12**. The y-axis represents the log of the rate constant for the reaction between the series of nucleophiles and electrophiles. The overall trend is as expected: as one moves right on the plot, the rate of the reaction increases. This

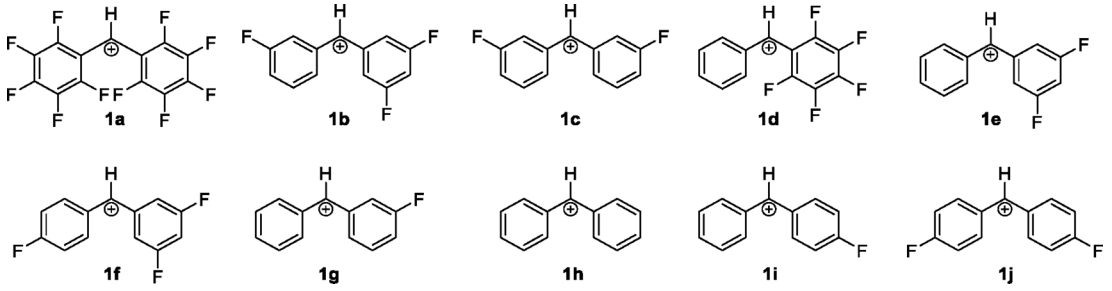

Figure 2. Substituted benzhydryl cation electrophiles studied herein.

https://doi.org/10.1021/acs.joc.1c02763
J. Org. Chem. 2022, 87, 1840−1849

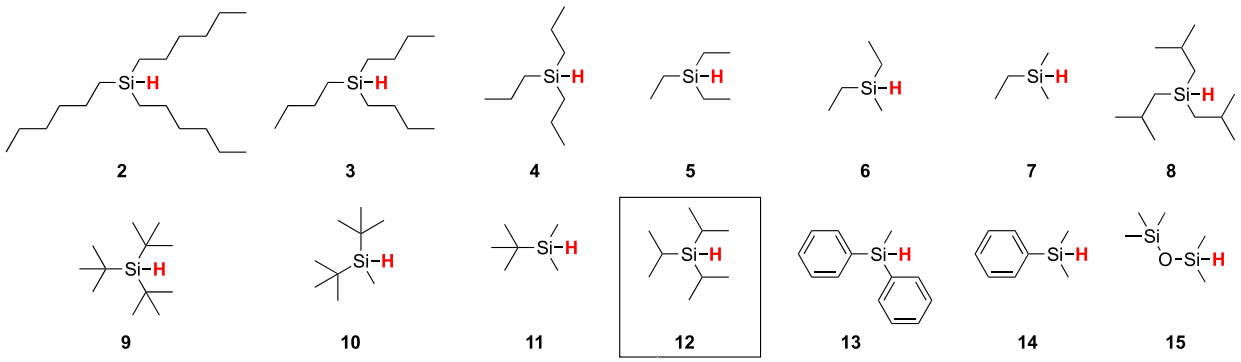

Figure 3. Substituted silanes studied herein. Boxed structure **12** represents the "reference" nucleophile (see the text).

makes sense because the electrophilicity of the benzhydryl cations increases when moving to the right.

Because of the large amount of data, we break down the discussion into different groups of silane substitutions.

Alkyl Chain Length. A Mayr-type plot of the silanes containing *n*-alkyl chain substitution is shown in Figure 8. For all of these types of plots, the linear fit equation and the correlation coefficient are listed in the Supporting Information. In general, we find that the silanes with shorter alkyl chain substitutions react more sensitively to electrophile variation: the lines for Et_3SiH (**5**), Et_2MeSiH (**6**), and $EtMe_2SiH$ (**7**) have steeper (more positive) slopes than the lines for $n$$Hex_3SiH$ (**2**), $n$$Bu_3SiH$ (**3**), and $n$$Pr_3SiH$ (**4**) (Figure 8).[40] Prior studies by Mayr have established that multiple factors may lead to sensitivity changes; our data indicate that in the gas phase, longer *n*-alkyl chain substitution leads to less sensitivity to electrophile variation.[17,18]

If we consider the trend for the triethyl, tri-*n*-propyl, tri-*n*-butyl, and tri-*n*-hexyl silanes (**5**, **4**, **3**, and **2**, respectively), we observe that the hydricity increases as the alkyl chain length increases [$n$$Et_3SiH$ **5** is the least nucleophilic in this group (which means it donates hydride most slowly), while $n$$Hex_3SiH$ **2** is generally the most nucleophilic (transfers hydride most quickly)].[41] We note that the specific rate constants do not always track perfectly with the trend line [for example, $n$$Hex_3SiH$ does not react the fastest with every cation (Table 1)]. However, the Mayr-type plot in Figure 8 does appear to show general trends that we discuss herein. The increasing rate of reaction with an increasing alkyl chain length makes intuitive sense; the silyl cation resulting from the removal of a hydride (Figure 1) would be stabilized by larger, more polarizable groups. To lend support to this hypothesis, we report our calculated polarizability for these silanes and find that greater polarizability is associated with greater hydricity (Table 3). We also list the σ_I inductive donor Taft parameters.[42−44] A more negative σ_I value indicates a more inductive donor; the trend therefore is consistent among increasing hydricity, increasing polarizability, and more negative σ_I values (**5** < **4** < **3** < **2**, where **2** is most nucleophilic).

If we focus on the silanes with ethyl and methyl substitution (triethyl-, diethyl methyl-, and ethyl dimethyl-substituted silanes **5**−**7**, respectively), different slopes result in different types of reactivity−selectivity relationships, depending on the identity of the electrophile (Figure 8). For less electrophilic benzhydryl cations, Et_2MeSiH (**6**) reacts more quickly than Et_3SiH (**5**). However, as the electrophiles become more electrophilic, the correlation lines cross and the reaction with Et_3SiH (**5**) becomes faster. This is also seen with Et_2MeSiH (**6**) and $EtMe_2SiH$ (**7**), although **6** reacts considerably faster than **7** with cations that have low electrophilicity, such that the correlation lines do not cross until very electrophilic cations are used.

Branching. To ascertain the effect of straight chain versus branching alkyl substituents, one can compare $n$$Pr_3SiH$ (**4**) with $i$$Pr_3SiH$ (**12**). These lines are not parallel (Figure 9), and the branched silane $i$$Pr_3SiH$ (**12**) is much more sensitive to electrophile variation than **4**, as indicated by the more positive slope for **12**. With low-electrophilicity cations, $n$$Pr_3SiH$ **4** is a better nucleophile (higher kinetic hydricity). However, for more strongly electrophilic cations, the triisopropyl-substituted silane **12** reacts more quickly and is thus a better hydride donor.

For the series $n$$Bu_3SiH$ (**3**), $i$$Bu_3SiH$ (**8**), and $t$$Bu_3SiH$ (**9**), we find that the sterically hindered **9** is by far the most sensitive to electrophile variation (Figure 10). The increased sensitivity of **9**, relative to those of both **3** and **8**, means that while **9** reacts more slowly in reactions with less electrophilic benzhydryl cations, it reacts more quickly with more electrophilic cations.

Thus, in terms of branching, the general trend is that silanes with an increased level of branching around the reactive center appear to be more sensitive to electrophile variation: $i$$Pr_3SiH$ (**12**) is more sensitive than $n$$Pr_3SiH$ (**4**, Figure 9), and $t$$Bu_3SiH$ (**9**) is more sensitive than $n$$Bu_3SiH$ (**3**, Figure 10).

Phenyl Substitution. Comparison of $MePh_2SiH$ **13** and Me_2PhSiH **14** indicates that the former is much less sensitive to electrophile variation (Figure 11). Therefore, with less electrophilic cations, $MePh_2SiH$ **13** is the better hydride donor, while with more electrophilic cations, Me_2PhSiH **14** reacts faster. The sensitivity of the silane that has an extra phenyl group may be decreased because phenyl substitution provides such good stabilization of the silyl cation resulting from hydride donation (Figure 1) that the nature of the benzhydryl cation electrophile is less important.

Silanes with the RMe_2SiH Formula. There are three RMe_2SiH compounds that do not contain an oxygen: $EtMe_2SiH$ (**7**), $t$$BuMe_2SiH$ (**11**), and $PhMe_2SiH$ (**14**). The data for these three species are plotted in Figure 12. In terms of sensitivity, the data for $t$$BuMe_2SiH$ (**11**) and $PhMe_2SiH$ (**14**) result in fairly parallel lines, indicating similar sensitivity. The reactions of the benzhydryl cations with $EtMe_2SiH$ **7** result in a line with a slightly steeper slope, indicating a higher sensitivity of **7** to the electrophile variation. $EtMe_2SiH$ **7** reacts most slowly and is most sensitive to the electrophile. The ranking for the rate of hydride transfer is **14** > **11** > **7**, which is consistent

https://doi.org/10.1021/acs.joc.1c02763
J. Org. Chem. 2022, 87, 1840−1849

Table 1. Gas-Phase Rate Constants k ($\times 10^{-10}$ cm^3 molecule^{-1} s^{-1}) for the Reactions of Benzhydryl Cations 1 with Silanes 2−15

	1a	1b	1c	1d	1e	1f	1g	1h	1i	1j
2	1.94 ± 0.99	2.03 ± 0.43	2.85 ± 0.91	2.51 ± 0.22	2.18 ± 0.42	3.08 ± 0.63	2.95 ± 0.57	1.00 ± 0.15	3.00 ± 0.50	1.07 ± 0.08
3	3.97 ± 0.90	2.92 ± 0.07	2.76 ± 0.26	2.14 ± 0.23	1.20 ± 0.08	2.52 ± 0.89	0.66 ± 0.08	1.18 ± 0.31	0.78 ± 0.07	0.51 ± 0.22
4	1.91 ± 0.54	1.55 ± 0.14	1.68 ± 0.40	1.80 ± 0.58	1.84 ± 0.87	1.49 ± 0.77	1.44 ± 0.64	0.67 ± 0.32	0.54 ± 0.17	0.26 ± 0.08
5	2.25 ± 0.61[a,b]	1.83 ± 0.11[a,b]	1.16 ± 0.20[a]	1.27 ± 0.11[a]	0.61 ± 0.17	0.57 ± 0.09[a]	0.20 ± 0.01	0.07 ± 0.01	too slow	too slow
6	0.83 ± 0.34	0.62 ± 0.10	0.60 ± 0.28	0.42 ± 0.06	0.29 ± 0.03	0.25 ± 0.04	0.22 ± 0.10	0.08 ± 0.01	too slow	too slow
7	0.97 ± 0.05	0.49 ± 0.02	0.32 ± 0.04	0.25 ± 0.01	0.23 ± 0.01	0.17 ± 0.01	0.04 ± 0.02	too slow	too slow	too slow
8	2.35 ± 0.90	2.70 ± 1.25	2.28 ± 0.93	2.29 ± 0.25	2.24 ± 0.81	2.18 ± 0.54	1.51 ± 0.51	0.92 ± 0.14	0.89 ± 0.02	0.51 ± 0.16
9	3.58 ± 0.11	2.90 ± 0.38	2.96 ± 0.27	3.06 ± 0.30	2.66 ± 0.03	1.43 ± 0.10	1.91 ± 0.16	0.37 ± 0.04	0.48 ± 0.20	0.13 ± 0.04
10	2.05 ± 0.07	3.71 ± 0.43	2.46 ± 0.35	1.64 ± 0.06	1.52 ± 0.26	1.55 ± 0.31	1.52 ± 0.60	0.49 ± 0.10	1.16 ± 0.09	0.20 ± 0.04
11	1.16 ± 0.19	1.48 ± 0.32	0.71 ± 0.07	0.70 ± 0.01	0.53 ± 0.03	0.44 ± 0.06	0.61 ± 0.17	0.10 ± 0.04	too slow	too slow
12	2.68 ± 0.21[a,b]	2.22 ± 0.18[a,b]	1.76 ± 0.25[a,b]	1.70 ± 0.15[a,b]	1.00 ± 0.13	0.82 ± 0.06[a,b]	0.42 ± 0.03	0.17 ± 0.05	0.16 ± 0.04	0.05 ± 0.01
13	2.80 ± 0.76	2.64 ± 0.39	2.54 ± 0.45	2.42 ± 0.69	2.36 ± 0.11	1.73 ± 0.23	2.52 ± 0.34	0.91 ± 0.18	1.46 ± 0.30	0.81 ± 0.10
14	4.13 ± 0.26[a]	3.47 ± 0.22[a]	3.09 ± 0.28[a,b]	2.76 ± 0.17[a]	1.90 ± 0.55	1.77 ± 0.44[a,b]	0.97 ± 0.10	0.46 ± 0.05	0.44 ± 0.06	0.24 ± 0.07
15	0.42 ± 0.11[a]	0.14 ± 0.08[a]	0.15 ± 0.02[a,b]	0.15 ± 0.04[a,b]	0.05 ± 0.03	0.07 ± 0.02[a,b]	too slow	too slow	too slow	too slow

[a]From ref 27. [b]Some values have been updated with additional measurements.

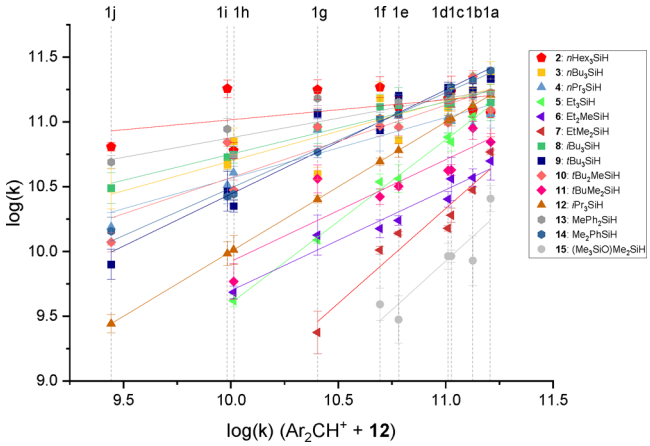

Figure 4. Rate constants for the reactions of benzhydryl cations with silanes **2**−**15**. The *y*-axis represents the log of the rate constants for the reactions of each electrophile with each nucleophile. The *x*-axis is the log of the rate constant of each electrophile with **12**.

with their polarizabilities (Table 4). In addition to polarizability, the phenyl group in **14** should stabilize the resultant silyl cation through resonance, as well, which explains its fast reaction.

Effect of Oxygen. Comparison of two silanes, one of which does not have an oxygen (**7**) and one of which does (**15**), indicates a similar sensitivity to electrophile variation (Figure 13). Furthermore, oxygen slows the hydride reaction. This is consistent with the inductively electron-withdrawing nature of oxygen, which renders Si−H cleavage less favorable, resulting in a considerable decrease in kinetic hydricity. Apparently, this outweighs any electron donation that oxygen could contribute to stabilize the resultant silyl cation (Figure 1).

One other general trend we notice, among these data, is that faster reactions tend to be less sensitive to the electrophile. There may be some correlation here, where when reactions accelerate, they are less selective.

Comparison of Gas-Phase Data to Mayr Condensed-Phase Data. We examined 10 silanes that were also examined by Mayr.[17,24,25] The advantage of studying these reactions in the gas phase and comparing their data to the condensed-phase data generated by Mayr is that any differences can be attributed to solvent effects. Interestingly, for the condensed-phase reactions, the sensitivity parameter s_N is fairly constant (~0.7). In other words, when the condensed-phase data are plotted following eq 2, the resultant lines are parallel. For our gas-phase studies, as noted in the prior section, the sensitivities of various silanes often differ, as evidenced by varying linear slopes. Thus, the silanes clearly show sensitivity differences in the gas phase (as evidenced by the different slopes in Figure 1) but not in solution. Solvent "dampens" or "equalizes" the inherent sensitivity differences. This result shows the importance of the gas-phase studies in ascertaining intrinsic reactivity that is modified by solvation.

Although sensitivities differ in the gas phase, we did want to find a way to compare the gas- and condensed-phase data; therefore, we chose an electrophile that reacts relatively quickly and was also studied by Mayr, **1b** (the 3,3′,5-trifluoro-substituted benzhydryl cation). In the condensed phase, the "*E*" value for this electrophile is 7.52; we used eq 2 to calculate the condensed-phase log(k). Our gas-phase "*E*" value for **1b** is 11.13, and we used our linear correlation to report a gas-phase

https://doi.org/10.1021/acs.joc.1c02763
J. Org. Chem. 2022, 87, 1840−1849

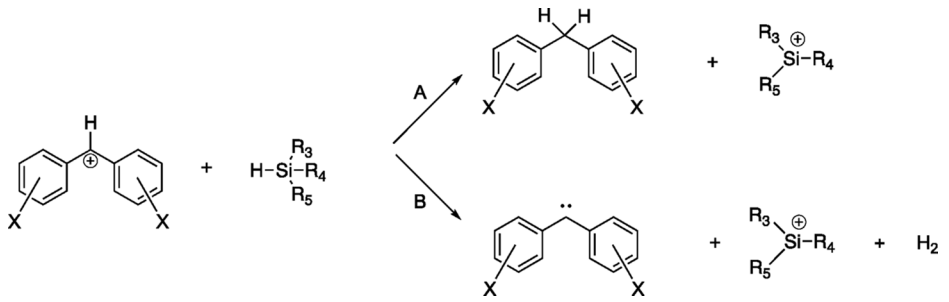

Figure 5. Hydride transfer vs proton abstraction.

Table 2. Free Energies (ΔG) of the Reaction between Benzhydryl Cation 1 and the Reference Silane (iPr$_3$SiH, 12) for Path A (hydride transfer) and Path B (proton abstraction) (Figure 5)[a]

	ΔG			
cation	path A[b]	path A[c]	path B[b,d]	path B[c,d]
1a (perfluoro)	−33.0	−32.0	+46.8 (+37.8)	+49.3 (+39.3)
1b (3,3′,5-trifluoro)	−15.7	−16.0	+60.7 (+53.3)	+61.8 (+53.6)
1c (3,3′-difluoro)	−10.6	−11.7	+65.1 (+57.8)	+65.4 (+57.7)
1d (pentafluoro)	−17.9	−18.1	+60.0 (+51.9)	+61.3 (+52.5)
1e (3,5-difluoro)	−10.7	−11.3	+64.7 (+57.7)	+65.5 (+57.9)
1f (3,4′,5-trifluoro)	−11.6	−12.1	+62.7 (+56.6)	+63.9 (+57.3)
1g (3-fluoro)	−5.7	−6.7	+69.1 (+62.3)	+69.7 (+62.2)
1h (unsubstituted)	−1.3[e]	−1.9	+73.2 (+66.6)	+74.0 (+66.3)
1i (4-fluoro)	−2.4	−3.2	+71.2 (+65.4)	+72.0 (+65.5)
1j (4,4′-difluoro)	−3.8	−4.2	+69.3 (+64.0)	+70.4 (+64.6)

[a]All values are in kcal mol^{-1}. [b]Calculated at B3LYP/6-31+G(d), at 298 K. [c]Calculated at B3LYP-D3(BJ)/6-311++G(2d,p), at 298 K. [d]To form the singlet carbene (triplet carbene). [e]From ref 27.

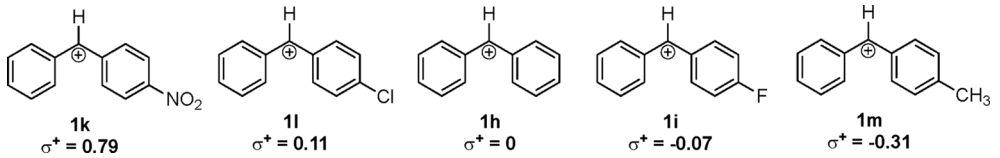

Figure 6. 4-Substituted benzhydryl cations used for Hammett studies and their σ^+ values.[37,38]

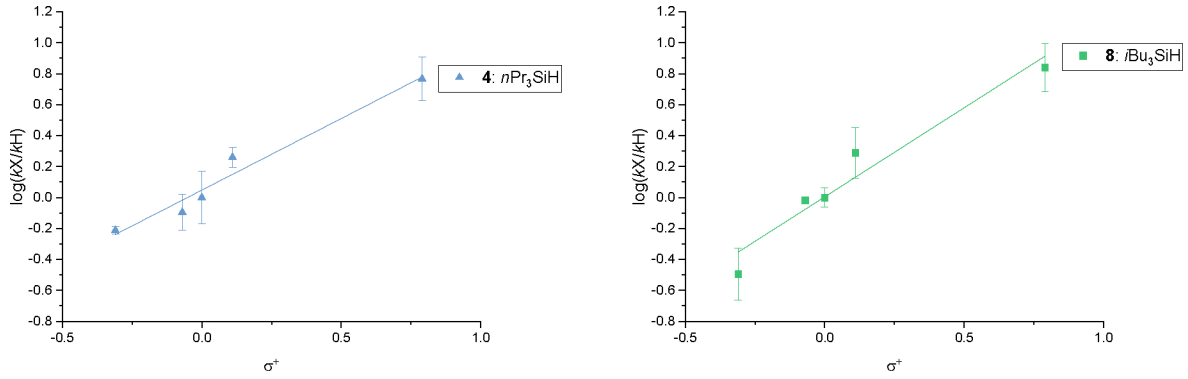

Figure 7. Hammett plots for the reactions of silanes **4** (left) and **8** (right) with benzhydryl cations in Figure 6.

log(k) (y value when x = 11.13 in the plots in Figure 4) (Table 5). The data in the table are in the order of decreasing condensed-phase values.

Determining where the gas- and condensed-phase data correlate, and where they do not, would be of interest. In terms of alkyl chain length, Mayr has found that for tri-*n*-alkyl-silanes in solution, generally, a longer alkyl chain length correlates to a faster reaction, just as we find in the gas phase (Table 6).[17,24,25] He notes that this is consistent with hydride abstraction being controlled by inductive, as opposed to steric, effects, as the trend parallels that of σ_I inductive donor Taft parameters (Table 6; a more negative σ_I value indicates a stronger inductive donor).[42−44,47] The correlation is not perfect; in both solution and the gas phase, nHex$_3$SiH **2** reacts slightly more slowly than expected, for this particular cation **1b**.

For the subgroups with ethyl and methyl substitution (**6** and **7**, respectively), the data in Table 5 show similar trends in the gas phase and in solution. Et$_2$MeSiH **6** reacts more quickly

https://doi.org/10.1021/acs.joc.1c02763
J. Org. Chem. 2022, 87, 1840−1849

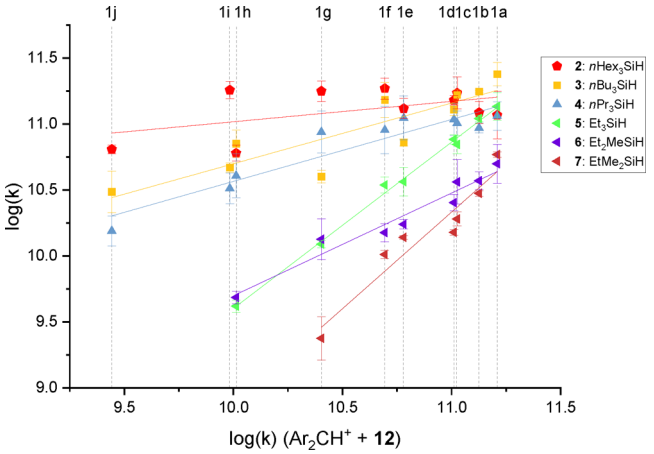

Figure 8. Rate constants for the reactions of benzhydryl cations with silanes that have *n*-alkyl chain substitution. The *y*-axis represents the log of the rate constants for the reactions of each electrophile with each nucleophile. The *x*-axis is the log of the rate constant of each electrophile with **12**.

Table 3. Silane Polarizabilities and Taft σ_I Parameters for 2−5

silane	polarizability ($\times 10^{-24}$ cm^3)[a]	Taft σ_I
2 (*n*Hex$_3$SiH)	37.7	−0.061[b]
3 (*n*Bu$_3$SiH)	25.8	−0.058[c]
4 (*n*Pr3SiH)	20.6	−0.057[d]
5 (*n*Et$_3$SiH)	15.0	−0.055[d]

[a]Calculated at B3LYP-D3(BJ)/6-311++G(2d,p), at 298 K. [b]From ref 44. [c]From ref 45. [d]From ref 42.

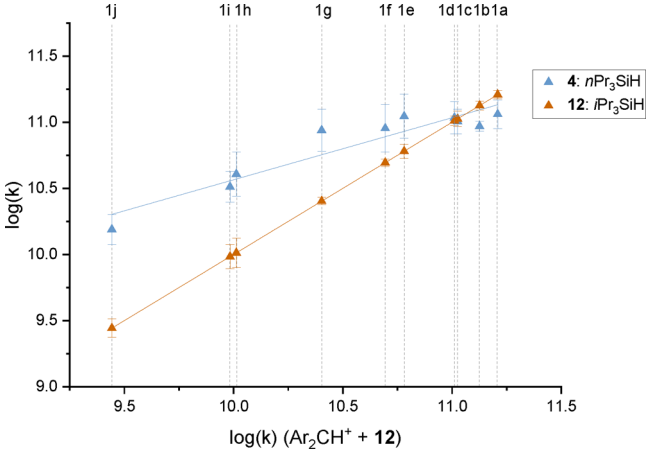

Figure 9. Rate constants for the reactions of benzhydryl cations with silanes that have branching and nonbranching propyl chain substitution. The *y*-axis represents the log of the rate constants for the reactions of each electrophile with each nucleophile. The *x*-axis is the log of the rate constant of each electrophile with **12**.

than EtMe$_2$SiH **7**.[17,24,25,46] This is consistent with both our calculated polarizability (13.1 and 11.3 × 10^{-24} cm^3 for **6** and **7**, respectively) and also what would be expected from the Taft σ_I parameter [ethyl is more inductively donating than methyl, so diethyl methyl silane **6** would be expected to be the better hydride donor, to form the most stable silyl cation product (Figure 1)].[42−44,47]

In terms of branching, Mayr finds that the *n*-alkyl silane *n*Pr$_3$SiH (**4**) reacts more rapidly than *i*Pr$_3$SiH (**12**). For us,

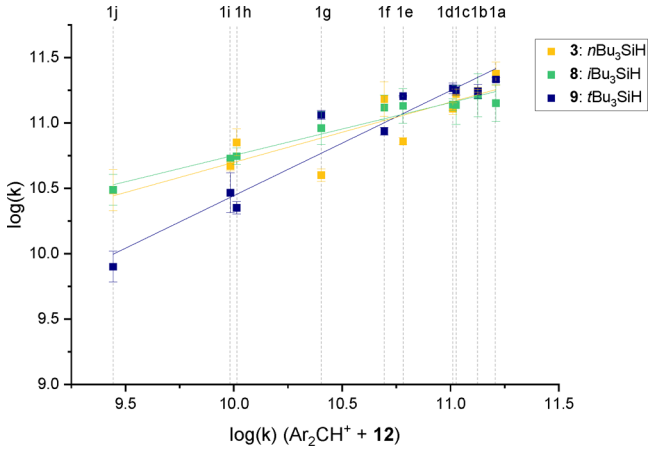

Figure 10. Rate constants for the reactions of benzhydryl cations with silanes that have branching and nonbranching butyl chain substitution. The *y*-axis represents the log of the rate constants for the reactions of each electrophile with each nucleophile. The *x*-axis is the log of the rate constant of each electrophile with **12**.

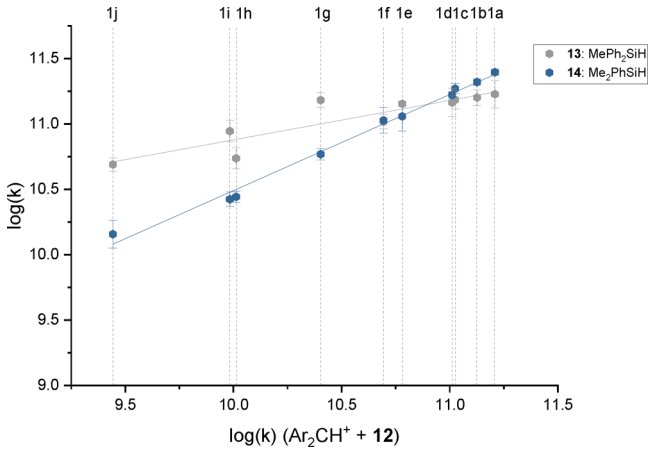

Figure 11. Rate constants for the reactions of benzhydryl cations with phenyl-containing silanes. The *y*-axis represents the log of the rate constants for the reactions of each electrophile with each nucleophile. The *x*-axis is the log of the rate constant of each electrophile with **12**.

because the *n*-propyl and isopropyl silanes have different sensitivities to the electrophiles (*vide supra*), we find that for more electrophilic cations, *i*Pr$_3$SiH (**12**) reacts more quickly than *n*Pr$_3$SiH (**4**); for the less electrophilic cations, we do see the same trend as Mayr [**4** reacts more quickly than **12** (Figure 9)]. For cation **1b** listed in Table 5, **12** and **4** have roughly the same rate constants in the gas phase. It thus would appear, as mentioned above, that the gas phase highlights a greater sensitivity to electrophile variation than does the condensed phase (because lines on our plots are not all parallel). Solvation is a more dominant factor that "equalizes" sensitivity, whereas in the gas phase, where intrinsic behavior can be seen, the inherent differences in the reactivity of the various silanes are more apparent.

We also noted previously, and note here again, that for Et$_3$SiH (**5**) and *i*Pr$_3$SiH (**12**), the former reacts more quickly in solution but the latter reacts faster in the gas phase.[27] The gas-phase results of **12** reacting more quickly than **5** are consistent with the increased polarizability (calculated to be 20.3 × 10^{-24} cm^3 for **12** but 15.0 × 10^{-24} cm^3 for **5**) as well as the Taft σ_I parameter (−0.064 for **12** and −0.055 for

https://doi.org/10.1021/acs.joc.1c02763
J. Org. Chem. 2022, 87, 1840−1849

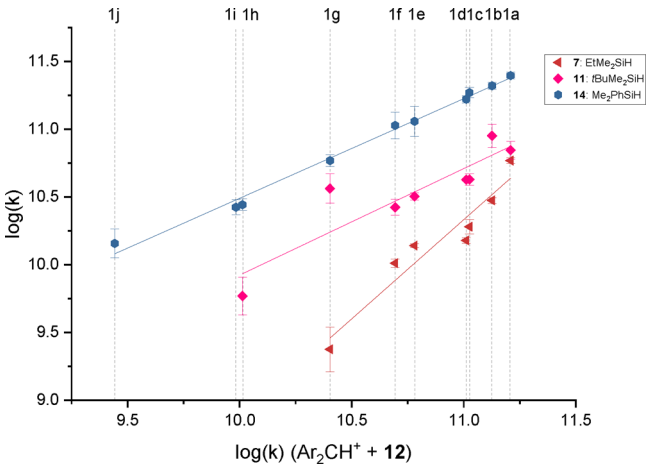

Figure 12. Rate constants for the reactions of benzhydryl cations with non-oxygen-containing silanes with the general formula RMe_2SiH (R = Et, tBu, or Ph). The *y*-axis represents the log of the rate constants for the reactions of each electrophile with each nucleophile. The *x*-axis is the log of the rate constant of each electrophile with **12**.

Table 4. Silane Polarizabilities for 7, 11, and 14

silane	polarizability ($\times 10^{-24}$ cm^3)[a]
14 ($PhMe_2SiH$)	17.8
11 ($tBuMe_2SiH$)	15.0
7 ($EtMe_2SiH$)	11.3

[a]Calculated at B3LYP-D3(BJ)/6-311++G(2d,p), at 298 K.

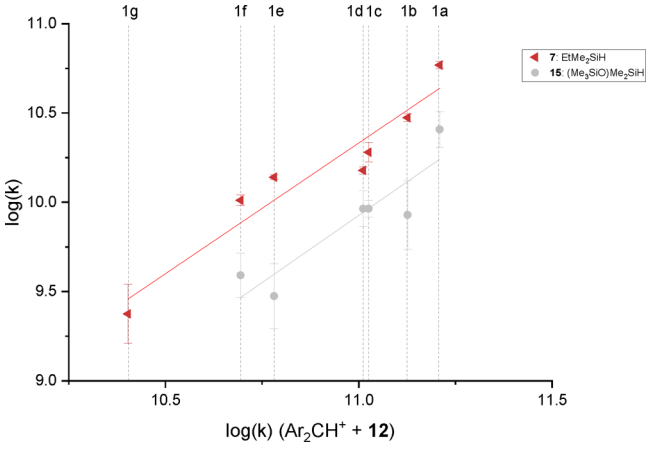

Figure 13. Rate constants for the reactions of benzhydryl cations with silanes with the general formula RMe_2SiH [R = Et or $O(SiMe_3)$]. The *y*-axis represents the log of the rate constants for the reactions of each electrophile with each nucleophile. The *x*-axis is the log of the rate constant of each electrophile with **12**.

Table 5. Comparison of Condensed- and Gas-Phase Log(k) Values

	silane	log(k) for reactions of silanes with **1b**, calculated using eq 2 (methylene chloride)[a]	log(k) for reactions of silanes with **1b** (gas phase)[b]
3	nBu_3SiH	8.40[c]	11.22
2	$nHex_3SiH$	8.33[c,d]	11.19
14	Me_2PhSiH	8.30[c]	11.32
4	nPr_3SiH	8.17[c,d]	11.10
6	Et_2MeSiH	7.97[c,d]	10.58
7	$EtMe_2SiH$	7.90[c]	10.52
5	Et_3SiH	7.78[c,e]	11.03
15	$(Me_3SiO)Me_2SiH$	7.77[c,d]	10.12
12	iPr_3SiH	7.63[d]	11.13
13	$MePh_2SiH$	7.48[d]	11.22

[a]The log(k) of the reaction is derived using eq 2 with **1b** (E = 7.52);[46] the units for the rate constants are M^{-1} s^{-1}. [b]This work. Log(k) for reaction of silanes with **1b** (see the text); the units for the rate constants are M^{-1} s^{-1} and are converted from cm^3 molecule^{-1} s^{-1} using a conversion factor of 6.022×10^{-26} molecule M^{-1} cm^{-3}. [c]From ref 25. [d]From ref 17. [e]From ref 24.

Table 6. Condensed- and Gas-Phase Reactions, Polarizabilities, and Taft Induction Parameters for nR_3SiH

R	log(k) for reactions of silanes with **1b**, calculated using eq 2 (methylene chloride)[a]	log(k) for reactions of silanes with **1b** (gas phase)[b]	polarizability of nR_3SiH ($\times 10^{-24}$ cm^3)[c]	σ_I for R
nHex (**2**)	8.33[d,e]	11.19	37.7	−0.061[g]
nBu (**3**)	8.40[d]	11.22	25.8	−0.058[h]
nPr (**4**)	8.17[d,e]	11.10	20.6	−0.057[i]
Et (**5**)	7.78[d,f]	11.03	15.0	−0.055[i]
Me	7.79[d,e]	N/A	9.6	−0.046[i]

[a]The log(k) of the reaction is derived using eq 2 and the s_N, N, and E values defined in the database.[36] [b]This work. Log(k) for the reaction of silanes with **1b** (see the text). [c]Calculated at B3LYP-D3(BJ)/6-311+G(2d,p), at 298 K. [d]From ref 25. [e]From ref 17. [f]From ref 24. [g]From ref 44. [h]From ref 45. [i]From ref 42.

5).[42−44,47] The reversal of the trend in solution, where **5** reacts more quickly than **12**, is similar to the well-known reversal in relative acidity between *tert*-butanol and methanol in solution as compared to the gas phase.[48] Therefore, it could be that here as well, in the gas phase, the reactivity is dominated by the stabilization of the resultant silyl cation after hydride abstraction by more polarizable, inductively donating groups (Figure 1). In solution, that stabilization may be mitigated by solvation; although the iPr_3Si^+ cation should be stabilized inherently, the poor solvation of the bulkier groups (relative to the Et_3Si^+ cation) may make the iPr_3SiH reaction less favorable. This result highlights the importance of intrinsic reactivity studies such as this.

The trends for the effect of a phenyl group and an oxygen are parallel in both the gas phase and solution. If we compare **14** ($PhMe_2SiH$) and **7** ($EtMe_2SiH$), we find that **14** reacts faster than **7** in both media. In both solution and the gas phase, oxygen also slows the reaction; **7** ($EtMe_2SiH$) reacts more quickly than **15** [$(Me_3SiO)Me_2SiH$].

One last comparison between the gas phase and solution is that the slowest reaction in solution is not the slowest in the gas phase. In solution, the slowest reacting silane in Table 5 is **13** (Ph_2MeSiH). This is by far not the slowest reaction in the gas phase. In fact, **13** is the second fastest reacting silane in the gas phase. We hypothesize that this significantly increased rate in the gas phase relative to that in the condensed phase may be due to the polarizability and resonance stabilization of the phenyl groups, which should stabilize the silyl cation formed after hydride abstraction (Figure 1). The noticeably high rate in the gas phase would indicate the intrinsic influence of the phenyl group in the absence of a solvent, which is mitigated significantly in solution.

https://doi.org/10.1021/acs.joc.1c02763
J. Org. Chem. 2022, 87, 1840−1849

To briefly summarize electrophilicity, the gas-phase trend is **1a** > **1b** > **1c** > **1d** > **1e** > **1f** > **1g** > **1h** > **1i** > **1j**, where **1a** is the most electrophilic. For the electrophiles that Mayr studied that overlap with ours, the trend is the same: **1b** > **1c** > **1e** > **1g** > **1h** > **1i** > **1j**. These results are consistent with the Mayr interpretation that electrophile solvation energies change proportionally with electrophilic reactivities; we therefore see this proportionality in the absence of a solvent.[46,49,50]

Last, in terms of absolute rate constants that were explicitly measured in both media, the gas-phase reactions are faster than those in solution, by ∼2000 times, highlighting the relative ease of reaction in the absence of a solvent.

CONCLUSIONS

This work represents significant progress toward developing a gas-phase hydricity scale. Kinetic hydricity is valuable both for the improved design of hydrides for alternate energy applications and, more broadly, for a deeper understanding of intrinsic nucleophilicity and electrophilicity. Our gas-phase results indicate that silanes substituted with longer *n*-alkyl chains are less sensitive to electrophile variation. Hydricity increases as alkyl chain length increases, consistent with polarizability and the Taft σ_I parameter. For silanes with branching alkyl groups, we find that in the gas phase, more branching leads to greater sensitivity to electrophile variation. Substitution of the silane with oxygen slows the reaction. When comparing the solution- and gas-phase results, we note that for both media, alkyl substitution results in increased hydricity. While the effect of phenyl and oxygen substitution is similar in solution and in the gas phase, we see an intriguing reversal in reactivity for Et_3SiH (**5**) and iPr_3SiH (**12**) in the gas phase versus solution. Perhaps the most striking difference is how in the gas phase, the sensitivity of the silanes to the electrophile variation changes, whereas in solution, the sensitivity tends to be quite constant. These intriguing similarities and differences in the speed and sensitivity of these reactions when gas and condensed phases are compared highlight the importance of this type of study. These results show the promise of being able to independently investigate electrophilicity and nucleophilicity in the gas phase and the ability to directly compare condensed-phase electrophile and nucleophile data. This represents a potential breakthrough in the understanding of organic reactivity, because many of the phenomena observed in electrophile−nucleophile studies in solution cannot be adequately interpreted without knowledge of inherent reactivity.[51]

EXPERIMENTAL SECTION

Benzhydryl alcohols (precursors for the benzhydryl cations **1**) and silanes (**2**−**15**) were all commercially available and used as received.

Fourier transform ion cyclotron resonance mass spectrometry (FTMS), with a 3.3 T magnetic field, was used to measure all of the rate constants reported herein. In this dual-cell setup (with a baseline pressure of 1×10^{-9} Torr), which has been reported in detail previously,[52,53] neutral substances can be added to either cell independently. Here, the solid benzhydryl alcohols were added to the "source" cell using a heatable solid probe, and the liquid silanes were added to the "analyzer" cell using a system of heatable batch inlets. Hydronium ions were formed by pulsing water into the cell and ionizing it using an electron beam (ranging from 20 to 30 eV, 4−6 μA, 0.5 s). These hydronium ions were then used to form the benzhydryl cations, **1**, via protonation of the benzhydryl alcohol (eq 3).

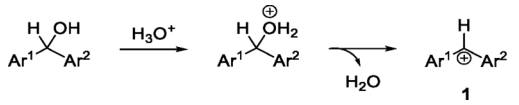

(3)

To perform the reaction, benzhydryl cations were first transferred from the "source" cell to the "analyzer" cell through a 2 mm wide hole in the middle trapping plate by briefly decreasing the voltage. Then, gas-phase rate constants were measured using pseudo-first-order conditions, where the concentration of the neutral silane in the "analyzer" cell was kept in excess relative to the concentration of the benzhydryl cations; this has also been described previously.[52,53] The concentration, or pressure, of the neutral silane in the analyzer cell was measured by using a fast control reaction (hydronium with silanes), because the pressure measurements from the ion gauges were not always accurate; this has also been described previously.[52−55]

All density functional theory calculations were conducted using Gaussian 09[56] and Gaussian 16[57] using the B3LYP/6-31+G(d) and B3LYP-D3(BJ)/6-311++G(2d,p) levels of theory.[58−62] All ground state geometries were fully optimized, and the resulting structures had no negative frequencies. Transition state structures were verified with frequency calculations and by identifying one imaginary frequency. No scaling factor was applied. Reported values are at 298 K.

ASSOCIATED CONTENT

Supporting Information

The Supporting Information is available free of charge at https://pubs.acs.org/doi/10.1021/acs.joc.1c02763.

Cartesian coordinates for all calculated species, linear regression analysis for all relevant figures, and additional experimental rate constants (PDF)

AUTHOR INFORMATION

Corresponding Author

Jeehiun K. Lee − *Department of Chemistry and Chemical Biology, Rutgers, The State University of New Jersey, New Brunswick, New Jersey 08901, United States;* orcid.org/0000-0002-1665-1604; Email: jee.lee@rutgers.edu

Author

Allison E. Krajewski − *Department of Chemistry and Chemical Biology, Rutgers, The State University of New Jersey, New Brunswick, New Jersey 08901, United States*

Complete contact information is available at: https://pubs.acs.org/10.1021/acs.joc.1c02763

Notes

The authors declare no competing financial interest.

ACKNOWLEDGMENTS

The authors thank the National Science Foundation (NSF) and the NSF Extreme Science and Engineering Discovery Environment (XSEDE) for support. The authors are also grateful to Professor Herbert Mayr for incredibly insightful discussions.

REFERENCES

(1) Hummel, W. Large-Scale Applications of NAD(P)-Dependent Oxidoreductases: Recent Developments. *Trends Biotechnol* **1999**, *17*, 487−492.

(2) Voet, D.; Voet, J. G. *Biochemistry*, 4th ed.; John Wiley & Sons, Inc.: New York, 2010.

(3) Waldie, K. M.; Ostericher, A. L.; Reineke, M. H.; Sasayama, A. F.; Kubiak, C. P. Hydricity of Transition-Metal Hydrides: Thermodynamic Considerations for CO_2 Reduction. *ACS Catal.* **2018**, *8*, 1313−1324. and references therein

(4) Brown, H. C.; Krishnamurthy, S. Forty Years of Hydride Reductions. *Tetrahedron* **1979**, *35*, 567−607.
(5) Brown, H. C.; Kim, S.; Krishnamurthy, S. Selective Reductions. 26. Lithium Triethylborohydride as an Exceptionally Powerful and Selective Reducing Agent in Organic Synthesis. Exploration of the Reactions with Selected Organic Compounds Containing Representative Functional Groups. *J. Org. Chem.* **1980**, *45*, 1−12.
(6) Stephan, D. W.; Erker, G. Frustrated Lewis Pair Chemistry: Development and Perspectives. *Angew. Chem., Int. Ed.* **2015**, *54*, 6400−6441.
(7) Stephan, D. W. Frustrated Lewis Pairs: From Concept to Catalysis. *Acc. Chem. Res.* **2015**, *48*, 306−316.
(8) Lim, C. H.; Holder, A. M.; Hynes, J. T.; Musgrave, C. B. Catalytic Reduction of CO_2 by Renewable Organohydrides. *J. Phys. Chem. Lett.* **2015**, *6*, 5078−5092.
(9) Fernández-Alvarez, F. J.; Oro, L. A. Homogeneous Catalytic Reduction of CO_2 with Silicon-Hydrides, State of the Art. *ChemCatChem.* **2018**, *10*, 4783−4796.
(10) Alherz, A.; Lim, C. H.; Kuo, Y. C.; Lehman, P.; Cha, J.; Hynes, J. T.; Musgrave, C. B. Renewable Hydride Donors for the Catalytic Reduction of CO_2: A Thermodynamic and Kinetic Study. *J. Phys. Chem. B* **2018**, *122*, 10179−10189.
(11) Lipke, M. C.; Liberman-Martin, A. L.; Tilley, T. D. Electrophilic Activation of Silicon−Hydrogen Bonds in Catalytic Hydrosilations. *Angew. Chem., Int. Ed.* **2017**, *56*, 2260−2294.
(12) Larson, G. L.; Fry, J. L. *Ionic and Organometallic-Catalyzed Organosilane Reductions*; John Wiley & Sons, 2009; Vol. *81*.
(13) Larson, G. L. *Silicon-Based Blocking Agents. Suplement to the Gelest-Catalog (ABCR) Silicon, Germanium & Tin Compounds, Metal Alkoxides and Metal Diketonates*; 2014.
(14) Ilic, S.; Alherz, A.; Musgrave, C. B.; Glusac, K. D. Thermodynamic and Kinetic Hydricities of Metal-Free Hydrides. *Chem. Soc. Rev.* **2018**, *47*, 2809−2836.
(15) Ilic, S.; Pandey Kadel, U.; Basdogan, Y.; Keith, J. A.; Glusac, K. D. Thermodynamic Hydricities of Biomimetic Organic Hydride Donors. *J. Am. Chem. Soc.* **2018**, *140*, 4569−4579.
(16) Brereton, K. R.; Smith, N. E.; Hazari, N.; Miller, A. J. M. Thermodynamic and Kinetic Hydricity of Transition Metal Hydrides. *Chem. Soc. Rev.* **2020**, *49*, 7929−7948.
(17) Mayr, H.; Basso, N. Kinetics of Hydride Transfers from CH, SiH, GeH, and SnH Groups to Carbenium Ions. *Angew. Chem., Int. Ed.* **1992**, *31*, 1046−1048.
(18) Mayr, H.; Patz, M. Scales of Nucleophilicity and Electrophilicity: A System for Ordering Polar Organic and Organometallic Reactions. *Angew. Chem., Int. Ed.* **1994**, *33*, 938−957.
(19) Mayr, H.; Bug, T.; Gotta, M. F.; Hering, N.; Irrgang, B.; Janker, B.; Kempf, B.; Loos, R.; Ofial, A. R.; Remennikov, G.; Schimmel, H. Reference Scales for the Characterization of Cationic Electrophiles and Neutral Nucleophiles. *J. Am. Chem. Soc.* **2001**, *123*, 9500−9512.
(20) Lucius, R.; Loos, R.; Mayr, H. Kinetic Studies of Carbocation−Carbanion Combinations: Key to a General Concept of Polar Organic Reactivity. *Angew. Chem., Int. Ed.* **2002**, *41*, 91−95.
(21) Minegishi, S.; Kobayashi, S.; Mayr, H. Solvent Nucleophilicity. *J. Am. Chem. Soc.* **2004**, *126*, 5174−5181.
(22) Mayr, H.; Ofial, A. R. Kinetics of Electrophile-Nucleophile Combinations: A General Approach to Polar Organic Reactivity. *Pure Appl. Chem.* **2005**, *77*, 1807−1821.
(23) Mayr, H.; Ofial, A. R. Do General Nucleophilicity Scales Exist? *J. Phys. Org. Chem.* **2008**, *21*, 584−595.
(24) Ammer, J.; Nolte, C.; Mayr, H. Free Energy Relationships for Reactions of Substituted Benzhydrylium Ions: from Enthalpy Over Entropy to Diffusion Control. *J. Am. Chem. Soc.* **2012**, *134*, 13902−13911.
(25) Horn, M.; Schappele, L. H.; Lang-Wittkowski, G.; Mayr, H.; Ofial, A. R. Towards a Comprehensive Hydride Donor Ability Scale. *Chem. - Eur. J.* **2013**, *19*, 249−263.
(26) Mayr, H. Reactivity Scales for Quantifying Polar Organic Reactivity: The Benzhydrylium Methodology. *Tetrahedron* **2015**, *71*, 5095−5111.
(27) Xu, J.; Krajewski, A. E.; Niu, Y.; Kiruba, G. S. M.; Lee, J. K. Kinetic Hydricity of Silane Hydrides in the Gas Phase. *Chem. Sci.* **2019**, *10*, 8002−8008.
(28) Some of these structures were calculated in ref 27 but are compiled for the first time here.
(29) Michelson, A. Z.; Petronico, A.; Lee, J. K. 2-Pyridone and Derivatives: Gas-Phase Acidity, Proton Affinity, Tautomer Preference, and Leaving Group Ability. *J. Org. Chem.* **2012**, *77*, 1623−1631.
(30) Michelson, A. Z.; Rozenberg, A.; Tian, Y.; Sun, X.; Davis, J.; Francis, A. W.; O'Shea, V. L.; Halasyam, M.; Manlove, A. H.; David, S. S.; Lee, J. K. Gas-Phase Studies of Substrates for the DNA Mismatch Repair Enzyme MutY. *J. Am. Chem. Soc.* **2012**, *134*, 19839.
(31) Michelson, A. Z.; Chen, M.; Wang, K.; Lee, J. K. Gas-Phase Studies of Purine 3-Methyladenine DNA Glycosylase II (AlkA) Substrates. *J. Am. Chem. Soc.* **2012**, *134*, 9622−9633.
(32) Chen, M.; Moerdyk, J. P.; Blake, G. A.; Bielawski, C. W.; Lee, J. K. Assessing the Proton Affinities of *N,N'*-Diamidocarbenes. *J. Org. Chem.* **2013**, *78*, 10452−10458.
(33) Wang, K.; Chen, M.; Wang, Q.; Shi, X.; Lee, J. K. 1,2,3-Triazoles: Gas Phase Properties. *J. Org. Chem.* **2013**, *78*, 7249−7258.
(34) Niu, Y.; Wang, N.; Munoz, A.; Xu, J.; Zeng, H.; Rovis, T.; Lee, J. K. Experimental and Computational Gas Phase Acidities of Conjugate Acids of Triazolylidene Carbenes: Rationalizing Subtle Electronic Effects. *J. Am. Chem. Soc.* **2017**, *139*, 14917−14930.
(35) Wang, N.; Lee, J. K. Gas-Phase and Ionic Liquid Experimental and Computational Studies of Imidazole Acidity and Carbon Dioxide Capture. *J. Org. Chem.* **2019**, *84*, 14593−14601.
(36) For the reaction of **1h** and **12**, path B is so endergonic that the free energy simply increases to the product (no barrier to reverse reaction).
(37) Ritchie, C. D.; Sager, W. F. An Examination of Structure-Reactivity Relationships. *Prog. Phys. Org. Chem.* **2007**, *2*, 323−400.
(38) Hansch, C.; Leo, A.; Taft, R. W. A Survey of Hammett Substituent Constants and Resonance and Field Parameters. *Chem. Rev.* **1991**, *91*, 165−195.
(39) We also previously examined kinetic isotope effects, which also support path A (ref 27).
(40) The linearity for trihexylsilane (**2**) is quite poor, but the slope is definitely small.
(41) The line for triethylsilane (**5**) is steeper than that for the other three linear alkyl chain silanes, but generally, the reactions for **5** with the benzhydryl cations are the slowest.
(42) Taft, R. W., Jr; Lewis, I. C. The General Applicability of a Fixed Scale of Inductive Effects. II. Inductive Effects of Dipolar Substituents in the Reactivities of m-and p-Substituted Derivatives of Benzene. *J. Am. Chem. Soc.* **1958**, *80*, 2436−2443.
(43) Taft, R. W.; Lewis, I. C. Evaluation of Resonance Effects on Reactivity by Application of the Linear Inductive Energy Relationship-IV: Hyperconjugation Effects of para-Alkyl Groups. *Tetrahedron* **1959**, *5*, 210−232.
(44) Levitt, L. S. The Alkyl Inductive Effect. I. Relations between σI*, σ* and ρI ρ* for H and Alkyl Groups; σI Values from the Size and Branching of R. *Zeitschrift für Naturforschung B* **1979**, *34*, 81−85.
(45) Levitt, L.; Levitt, B. A Correlation of Ionisation Energies of Water and Alcohols with Polar and Inductive Substituent Constants. *Experientia* **1970**, *26*, 1183.
(46) Mayr, H. Mayr's Database of Reactivity Parameters. http://www.cup.lmu.de/oc/mayr/reaktionsdatenbank/ (accessed December 2021).
(47) Dayal, S.; Ehrenson, S.; Taft, R. Substituent Effects, Electronic Transmission, and Structural Dependence of Pi Delocalization as Studied with the *p*-Fluorophenyl Tag. *J. Am. Chem. Soc.* **1972**, *94*, 9113−9122.
(48) Brauman, J. I.; Blair, L. K. Gas-Phase Acidities of Alcohols. *J. Am. Chem. Soc.* **1970**, *92*, 5986−5992.
(49) Mayr, H.; Kempf, B.; Ofial, A. R. Π-Nucleophilicity in Carbon-Carbon Bond-Forming Reactions. *Acc. Chem. Res.* **2003**, *36*, 66−77.

https://doi.org/10.1021/acs.joc.1c02763
J. Org. Chem. 2022, 87, 1840−1849

(50) Denekamp, C.; Sandlers, Y. Electrophilicity-Nucleophilicity Scale Also in the Gas Phase. *Angew. Chem., Int. Ed.* **2006**, *45*, 2093−2096.
(51) Mayr, H.; Ofial, A. R. Philicities, Fugalities, and Equilibrium Constants. *Acc. Chem. Res.* **2016**, *49*, 952−965.
(52) Sharma, S.; Lee, J. K. Gas Phase Acidity Studies of Multiple Sites of Adenine and Adenine Derivatives. *J. Org. Chem.* **2004**, *69*, 7018−7025.
(53) Zhachkina, A.; Liu, M.; Sun, X.; Amegayibor, F. S.; Lee, J. K. Gas Phase Thermochemical Properties of the Damaged Base O^6-Methylguanine versus Adenine and Guanine. *J. Org. Chem.* **2009**, *74*, 7429−7440.
(54) Chesnavich, W. J.; Su, T.; Bowers, M. T. Collisions in a Noncentral Field: A Variational and Trajectory Investigation of Ion-Dipole Capture. *J. Chem. Phys.* **1980**, *72*, 2641−2655.
(55) Su, T.; Chesnavich, W. J. Parametrization of the Ion-Polar Molecule Collision Rate Constant by Trajectory Calculations. *J. Chem. Phys.* **1982**, *76*, 5183−5185.
(56) Frisch, M. J.; Trucks, G. W.; Schlegel, H. B.; Scuseria, G. E.; Robb, M. A.; Cheeseman, J. R.; Scalmani, G.; Barone, V.; Mennucci, B.; Petersson, G. A.; Nakatsuji, H.; Caricato, M.; Li, X.; Hratchian, H. P.; Izmaylov, A. F.; Bloino, J.; Zheng, G.; Sonnenberg, J. L.; Hada, M.; Ehara, M.; Toyota, K.; Fukuda, R.; Hasegawa, J.; Ishida, M.; Nakajima, T.; Honda, Y.; Kitao, O.; Nakai, H.; Vreven, T.; Montgomery, J. A., Jr.; Peralta, J. E.; Ogliaro, F.; Bearpark, M.; Heyd, J. J.; Brothers, E.; Kudin, K. N.; Staroverov, V. N.; Kobayashi, R.; Normand, J.; Raghavachari, K.; Rendell, A.; Burant, J. C.; Iyengar, S. S.; Tomasi, J.; Cossi, M.; Rega, N.; Millam, J. M.; Klene, M.; Knox, J. E.; Cross, J. B.; Bakken, V.; Adamo, C.; Jaramillo, J.; Gomperts, R.; Stratmann, R. E.; Yazyev, O.; Austin, A. J.; Cammi, R.; Pomelli, C.; Ochterski, J. W.; Martin, R. L.; Morokuma, K.; Zakrzewski, V. G.; Voth, G. A.; Salvador, P.; Dannenberg, J. J.; Dapprich, S.; Daniels, A. D.; Farkas, Ö.; Foresman, J. B.; Ortiz, J. V.; Cioslowski, J.; Fox, D. J. *Gaussian09*, rev. A.02; Gaussian, Inc.: Wallingford, CT, 2009.
(57) Frisch, M. J.; Trucks, G. W.; Schlegel, H. B.; Scuseria, G. E.; Robb, M. A.; Cheeseman, J. R.; Scalmani, G.; Barone, V.; Petersson, G. A.; Nakatsuji, H.; Li, X.; Caricato, M.; Marenich, A. V.; Bloino, J.; Janesko, B. G.; Gomperts, R.; Mennucci, B.; Hratchian, H. P.; Ortiz, J. V.; Izmaylov, A. F.; Sonnenberg, J. L.; Williams-Young, D.; Ding, F.; Lipparini, F.; Egidi, F.; Goings, J.; Peng, B.; Petrone, A.; Henderson, T.; Ranasinghe, D.; Zakrzewski, V. G.; Gao, J.; Rega, N.; Zheng, G.; Liang, W.; Hada, M.; Ehara, M.; Toyota, K.; Fukuda, R.; Hasegawa, J.; Ishida, M.; Nakajima, T.; Honda, Y.; Kitao, O.; Nakai, H.; Vreven, T.; Throssell, K.; Montgomery, J. A., Jr.; Peralta, J. E.; Ogliaro, F.; Bearpark, M. J.; Heyd, J. J.; Brothers, E. N.; Kudin, K. N.; Staroverov, V. N.; Keith, T. A.; Kobayashi, R.; Normand, J.; Raghavachari, K.; Rendell, A. P.; Burant, J. C.; Iyengar, S. S.; Tomasi, J.; Cossi, M.; Millam, J. M.; Klene, M.; Adamo, C.; Cammi, R.; Ochterski, J. W.; Martin, R. L.; Morokuma, K.; Farkas, O.; Foresman, J. B.; Fox, D. J. *Gaussian16*, rev. C.01; Gaussian, Inc.: Wallingford, CT, 2016.
(58) Lee, C.; Yang, W.; Parr, R. G. Development of the Colle-Salvetti Correlation-Energy Formula into a Functional of the Electron Density. *Phys. Rev. B* **1988**, *37*, 785−789.
(59) Becke, A. D. Density-Functional Thermochemistry. III. The Role of Exact Exchange. *J. Chem. Phys.* **1993**, *98*, 5648−5652.
(60) Becke, A. D. A. New Mixing of Hartree-Fock and Local Density-Functional Theories. *J. Chem. Phys.* **1993**, *98*, 1372−1377.
(61) Stephens, P. J.; Devlin, F. J.; Chabalowski, C. F.; Frisch, M. J. Ab Initio Calculation of Vibrational Absorption and Circular-Dichroism Spectra Using Density-Functional Force-Fields. *J. Phys. Chem.* **1994**, *98*, 11623−11627.
(62) Grimme, S. Semiempirical GGA-Type Density Functional Constructed with a Long-Range Dispersion Correction. *J. Comput. Chem.* **2006**, *27*, 1787−1799.

https://doi.org/10.1021/acs.joc.1c02763
J. Org. Chem. 2022, 87, 1840−1849